Transient Brain Activity Explains the Spectral Content of Steady-State Visual Evoked Potentials

Antoine Gaume, *EMBS Student Member*, François Vialatte, and Gérard Dreyfus, *IEEE Fellow*

Abstract— **Steady-state visual evoked potentials (SSVEPs) are widely used in the design of brain-computer interfaces (BCIs). A lot of effort has therefore been devoted to find a fast and reliable way to detect SSVEPs. We study the link between transient and steady-state VEPs and show that it is possible to predict the spectral content of a subject's SSVEPs by simulating trains of transient VEPs. This could lead to a better understanding of evoked potentials as well as to better performances of SSVEP-based BCIs, by providing a tool to improve SSVEP detection algorithms.**

I. Introduction

Visual evoked potentials (VEPs) are electric potentials elicited in the brain by sudden visual stimulation. When measured by electroencephalography (EEG) in single trial scenarios, these low amplitude signals (about 10 µV) are not easily discriminated from the rest of the recorded electric activity (i.e. the combination of other brain signals, electromyographic artifacts and electrical noise). Therefore, VEP waveforms are usually extracted by signal averaging of several trials starting at the presentation of the visual stimulus and lasting longer than the evoked response. The clinical standards for VEP recording and testing can be found for instance in Odom et al. (2009) [1].

Characteristics of VEPs can vary from subject to subject. For example, the functional integrity of the visual pathway is well known to influence the delay between the stimulation and the response of the visual cortex [1]. This property makes VEPs useful in clinical ophthalmology to diagnose possible lesions of the optic nerve. However, this functional integrity is only one of the factors that may explain the shape of a given evoked potential. Other factors include the parameters of the stimulus (shape, position and color), its physical properties (such as the response time and contrast of the display or the luminance of the stimulation) [2] as well as the position of the EEG electrodes, and of course, the inter-subject variability.

The shape of the VEP also changes when the stimulation is repeated periodically over time, in which case it is known as steady-state VEPs or SSVEPs. This definition of SSVEPs is widely accepted in the engineering community and matches the definition of Regan (1989) [3], who defined SSVEPs as the idealized response made by repetition of VEPs, whose frequency components remain constant in amplitude and phase over a long time period. It can be noted that Di Russo et al. (2003) [4] consider that VEPs are to be called steady-state only when the visual stimuli are presented rapidly enough to prevent the brain response from returning to base line state (i.e. when the inter-stimulation period is shorter than the VEP). Similarly, in [1], Odom considers that repetitive evoked potentials are to be considered steady-state at rapid rates of stimulation, when the recorded waveform becomes approximately sinusoidal. We will stick to the first definition and consider that SSVEPs can theoretically exist at any stimulation frequency.

These SSVEPs are widely used in the engineering domain to design brain-computer interfaces (BCIs) [5], where the frequency of an attended flickering stimulus is detected using EEG and translated into a command by the computer. They are also used in several cognitive neuroscience studies as well as in clinical studies (see Vialatte et al. (2010) [5] for a review). The advantage of SSVEPs is that they are elicited by a periodic stimulation and therefore are themselves periodic: their spectral content is located around the frequency of the stimulation and its multiples (called harmonics). SSVEPs are also more stationary than most of EEG activity [5], which means that their characteristics remain more constant over time. Thanks to this property, they can be easily detected using simple frequency analysis methods. This is why SSVEPs are generally studied in the frequency domain while transient VEPs are observed in the time domain.

In this study, we attempt to explain the origins of the spectral content of SSVEPs. Our working hypothesis is that the characteristics of SSVEPs in the frequency domain may be largely predicted from the average VEP generated with analog stimulation. To the best of our knowledge, the relationship between the time-frequency properties of VEPs and SSVEP responses has never been investigated. We therefore study the link between the intrinsic frequencies comprised in the transient VEP and the amplitudes of the harmonics of SSVEPs. Based on the hypothesis that SSVEPs are a succession of VEPs, we also propose a simulation method to predict these amplitudes at any stimulation frequency. We will make sure to identify the frequency domains in which these predictions are accurate.

II. Materials and Methods

A. Subjects

Ten healthy subjects took part in the experiment. Nine were males and one female, with an average age of 24.8 (standard deviation: 3.6, range: 21-34). All had normal or corrected-to-normal vision and none of them had any history

A. Gaume, F. Vialatte and G. Dreyfus are with the SIGMA Laboratory, ESPCI ParisTech; 10, rue Vauquelin, 75005 Paris, France (phone: +331 40 79 45 41; fax: +331 40 79 45 53; email: antoine.gaume@espci.fr).

A. Gaume is with the UPMC Univ. Paris 06, IFD; 4, Place Jussieu, 75005 Paris, France.

of epilepsy, migraine or any other neurological condition. The study followed the principles outlined in the Declaration of Helsinki. All participants were given explanations about the nature of the experiment and signed an informed consent form before the experiment started.

B. Experimental Conditions

EEG recordings took place in a dark room, where subjects were seated in a comfortable armchair, at about 70 cm from the screen used to display visual stimulation. The subjects were shown their EEG activity prior to the recording and explanations were given about muscular artifacts and eye blinks. They were instructed to relax and prevent excessive muscular contractions or eye movements.

C. Data Acquisition

EEG signals were continuously recorded at a sampling rate of 2 kHz using 16 active Ag/AgCl electrodes from an actiCap system, connected to a V-Amp amplifier, both from Brain Products. The electrodes were placed according to the 10-20 system with a focus on parietal and occipital regions at positions Fp1, Fp2, F7, F3, F4, F8, C3, C4, P7, P3, Pz, P4, P8, O1, Oz and O2. Two additional electrodes were used as ground and reference for the amplifier and were located respectively at AFz and FCz.

A photodiode connected directly to the EEG amplifier auxiliary input allowed synchronization between the EEG recordings and the visual stimulation. The BPW-21R photodiode was chosen for its sensitivity to visible light (420-675 nm) and its theoretical response time of about 3 µs, lower than any other time scale in our setup.

D. Stimulation

The presented stimuli were flickering black and white checkerboards composed of a 10 by 10 grid of squares, for a total stimulus size of 500 by 500 pixels, corresponding approximately to 11° by 11° of the visual field. During experiments, subjects were asked to keep their gaze on a 14 pixels red fixation cross located at the center of the display, at the intersection of four checkerboards.

Stimulations were designed using PsychToolBox-3 [6][7] on MATLAB and displayed on a Samsung S23A750D screen with a refresh rate of 120 Hz, allowing for more different stimulation frequencies than screens with lower refresh rates. It is generally considered that each reversal of a checkerboard produce the same evoked potential, so that a 120 Hz screen can display all stimulation frequencies submultiple of 120 Hz. In the rest of the paper, a stimulation with 2 reversals per second will be referred to as a 2 Hz stimulation, even though the flickering rate of each square of the pattern is 1 Hz. Photodiode measurements allowed us to check that the contrast of stimulations decreased by less than 1% between low frequency and high frequency stimulations (up to 60 Hz). Furthermore, the stimulation frequency had no noticeable variations over time at a 2 kHz sampling rate.

E. Experimental Procedure

Each experiment consisted in the recording of 2 minutes of resting state with eyes open, 2 minutes of resting state with eyes closed, a total of 5 minutes of VEPs (at a 2 Hz frequency) and 3 sets of SSVEPs, composed of 20 different stimulation frequencies, each presented during 15s in a randomized order, for a total of 45s of SSVEP signal per frequency. The total stimulation time was 20 minutes.

The sequences were displayed in the following order:

- 1 min resting state with eyes open
- 1 min resting state with eyes closed
- 5 sequences of 30 s of VEP recording (2 Hz)
- 20 sequences of SSVEP recording of 15 s each
- 20 sequences of SSVEP recording of 15 s each
- 20 sequences of SSVEP recording of 15 s each
- 1 min resting state with eyes open
- 1 min resting state with eyes closed
- 5 sequences of 30s of VEP recording (2Hz)

Between each sequence, the subject was able to rest for as long as desired, and controlled the beginning of the next sequence with a button. After the button was pressed, a 3s countdown preceded the beginning of the sequence.

SSVEPs were recorded at the following frequencies (in reversals per second): 1, 1.5, 2, 2.5, 3, 4, 5, 6, 7.05, 8, 9.23, 10, 12, 13.33, 15, 17.14, 20, 24, 30 and 40.

F. Signal Processing

Analyses were performed using MATLAB® 2013a, with the signal processing toolbox and the wavelet toolbox. The recorded EEG signals were filtered between 0.5 Hz and 90 Hz, and a notch filter was applied in real time by the amplifier to remove the 50 Hz component due to the power grid. Before any analysis was performed, all data were downsampled from 2 kHz to 1.8 kHz using MATLAB's resample function. Thanks to this procedure, all inter-stimuli durations for all previously mentioned frequencies corresponded to integer numbers of points in the downsampled signals. This allowed for precise segmentation of SSVEPs and precise estimation of frequencies using Fast Fourier Transform (FFT). Both filtering and downsampling were applied on the raw signal before any segmentation to avoid border effects.

G. Frequency and Time-Frequency Analyses

Estimation of the frequency components of a signal were made using MATLAB's FFT algorithm on time windows corresponding to multiples of the stimulation period, so that stimulation frequency and its harmonics would fall precisely on points of the resulting frequency axis. For SSVEP responses, the magnitude of the FFT is generally preferable to other power spectrum estimation methods (such as Welch's periodogram or multitapers) since SSVEP peaks are very precisely located in the frequency domain and are supposed to have a nearly constant phase as long as the stimulation frequency is stable.

Time-frequency decompositions were computed using MATLAB's wavelet toolbox. We used complex Morlet wavelets with 3 and 11 oscillations (respectively 'cmor1-1' and 'cmor1-3' in MATLAB). Magnitudes of time-frequency maps were kept for analysis.

H. Simulations

For a given frequency, SSVEPs were simulated for each subject by generating trains of individual VEPs. Delay between two successive waveforms was taken equal to the desired SSVEP period. When this delay was shorter than the length of the VEP, the waveforms were summed in the overlapping area. Fig. 1 illustrates the principle of this simulation and shows examples of SSVEPs simulated at different frequencies.

When the delay between the VEPs was so short that the main components of consecutive VEPs started to overlap one with another (N65, P90 and N180; see Fig. 2a), we applied a correction to the simulation process. The idea behind this correction is that the neuronal assembly responsible for VEP generation should not be able to give rise to two VEPs at the same time. Therefore, we considered that if the VEP waveform overlaps with the next VEP by 30%, then only 70% of the neurons can be involved in each VEP generation, thus multiplying the simulated SSVEP amplitude by 0.7. Since most of the VEP energy is generally contained in a 100 ms oscillation, this correction only affected simulations above 10 Hz. Practically, simulated SSVEPs were multiplied by 10 and divided by their stimulation frequency. Results of the simulation with and without this correction are presented and discussed in the following sections.

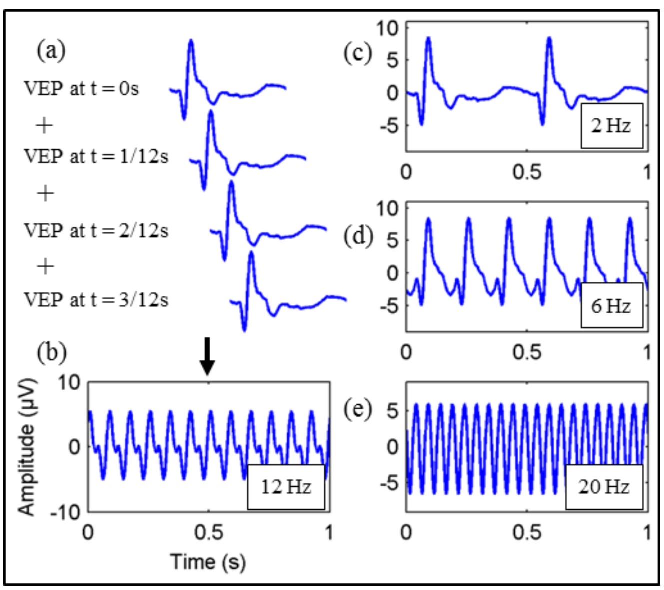

Figure 1. Simulation of SSVEPs using transient VEPs. (a) Principles of the simulation: in order to generate a SSVEP signal at a given frequency f, VEPs are concatenated in the time domain with a delay between two consecutive VEPs equal to the period of the stimulation (1/f). (b) Result of the simulation procedure at 12 Hz in the time domain. (c), (d), (e) SSVEPs simulated at other frequencies (2 Hz, 6 Hz and 20 Hz)

III. Results

A. VEP intrinsic components and SSVEPs

Fig. 2a shows the average VEP obtained on all subjects in the occipital region. The observed waveform is consistent with the expected VEP for pattern reversal stimulation as described in Odom et al. (2009) [1]. However, a notable difference can be observed: the N135 component described in [1] is shifted to 180 ms in our experiment. Fig. 2b shows the intrinsic time-frequency components of the average VEP computed using wavelet transform. It shows that the average VEP is composed of three main oscillatory bursts centered at (80 ms, 16 Hz), (110 ms, 7.5 Hz) and (190 ms, 3 Hz). Fig. 2c shows the average SSVEPs spectrum of subjects under a 2 Hz flickering checkerboard stimulation, recorded over the occipital region. The sharp vertical peaks correspond to the harmonics of the stimulation frequencies (every 2 Hz from 2 Hz to 30 Hz). It can be observed that harmonics at 14 Hz and 16 Hz are stronger than the neighboring peaks and that the overall localization of peaks (2-30 Hz) corresponds to the frequency domain of the VEP oscillatory bursts (Fig. 2b).

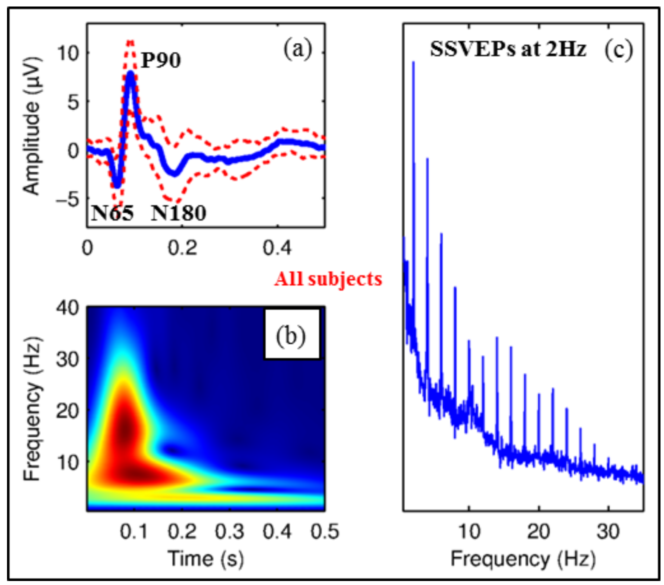

Figure 2. Average VEP and SSVEPs on all subjects. (a) VEP obtained in the occipital region (electrodes O1, Oz and O2) by averaging VEPs obtained on all subjects. Dashed lines: VEP ± standard deviation. Main components are N65 (negative at 65ms), P90 (positive at 90ms) and N180 (negative at 180ms). (b) Magnitude of the wavelet transform of the average VEP obtained using 3 oscillations wavelets described in [II. *G.*] (c) Average spectrum obtained by FFT of the brain response to a 2 Hz flickering stimulation in the occipital region. The sharp peaks observed at regular intervals correspond to the harmonics of the stimulation frequency.

While Fig. 2 focused on brain responses averaged on all subjects, Fig. 3 illustrates that individual VEPs obtained on a given subject can be used to explain the spectral content of that subject's SSVEPs. Occipital VEP, time-frequency decomposition of this VEP and SSVEPs at 2 and 3 Hz are shown for subject 4 (Fig. 3a) and 6 (Fig. 3b).

On the time-frequency map obtained from subject 4's VEP (Fig. 3a), strong components can be observed in the 3-14 Hz frequency band, as well as a moderate burst centered at 21 Hz with a hole around 15 Hz. Similarly, SSVEPs

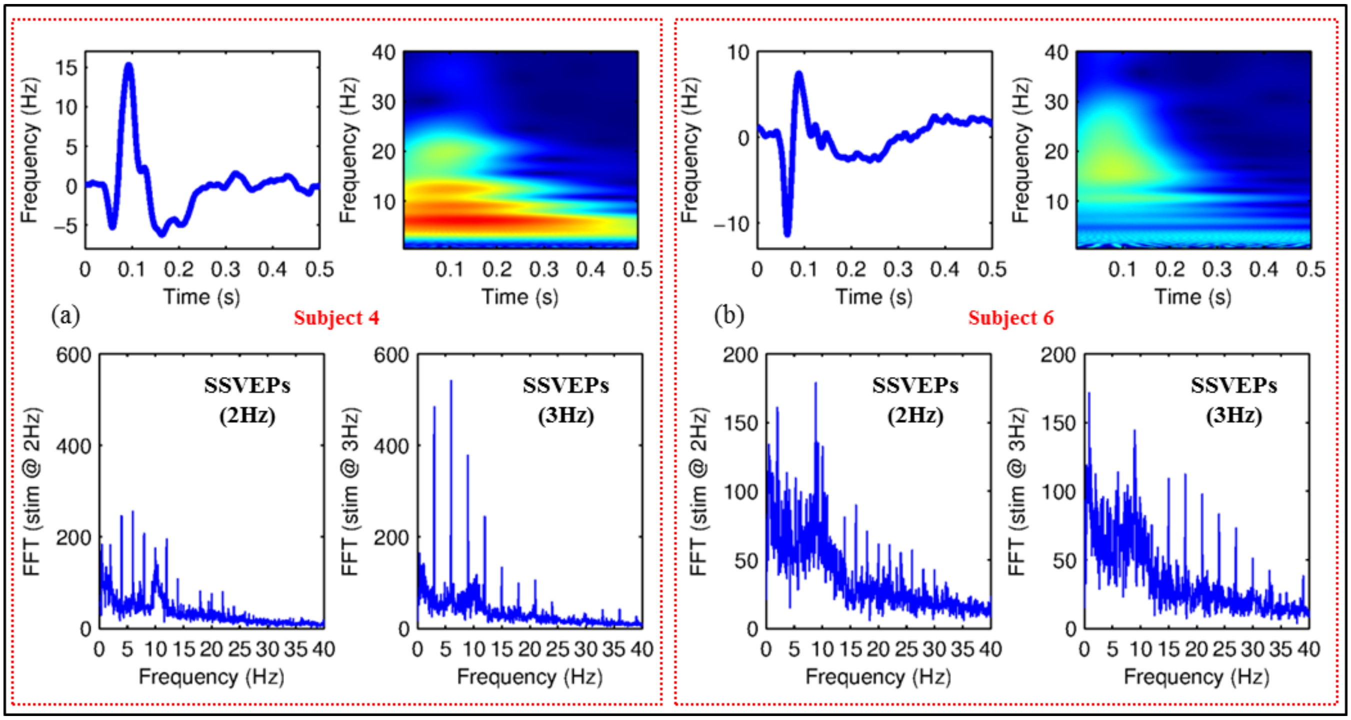

Figure 3. Illustration of the inter-subject variability. (a) Average VEP, wavelet transform and SSVEPs at 2 Hz and 3 Hz stimulation frequencies for subject 4 in the occipital region. Wavelet transform uses the 11 oscillations wavelet described in [II. *G.*] in order to increase frequency resolution (at the cost of time resolution). (b) Same as (a) for subject 6. FFTs are scaled for each subject to maximize readability but time-frequency maps have the same color axis (low amplitude = blue, high amplitude = red) and can be compared quantitatively.

contain strong harmonics below 15Hz and weak harmonics are visible in the 18-24 Hz range, with a decrease in harmonics amplitude around 15 Hz. A weak burst is observed in the VEP centered at (90 ms, 36 Hz), and, similarly, weak components can be found in the 3 Hz SSVEPs spectrum at 33, 36 and 39 Hz. Subject 6 (Fig. 3b) exhibits a different behavior: its VEP contains very little activity below 10 Hz, a narrow component at about 11 Hz and an important oscillatory burst ranging mostly from 14 Hz to 30 Hz, with small amplitude reaching frequencies above 40Hz. FFT of SSVEPs shows consistent results, with no or very weak peaks below 10 Hz, and strong amplitudes in the 14-30 Hz band.

B. *Simulation of SSVEPs using transient VEP*

Fig. 4 shows the results of the simulation process at different frequencies, with and without the correction described in [II. *H.*]. These results are averaged on all subjects. Without correction, quantitative prediction seems very accurate at low frequency (3 Hz is shown on the figure), and the accuracy of the simulation decreases when the frequency increases. Correction of the simulated amplitudes above 10 Hz gives good results at 15 and 20 Hz.

The accuracy of the simulation was estimated by averaging the squared differences between the experimental and simulated SSVEP peaks:

$$distance\,(f) = \frac{1}{nPeaks} \sum_{\substack{k \in [1;20] \\ kf < 40Hz}} \left(FFT_{exp}(kf) - FFT_{sim}(kf) \right)^2$$

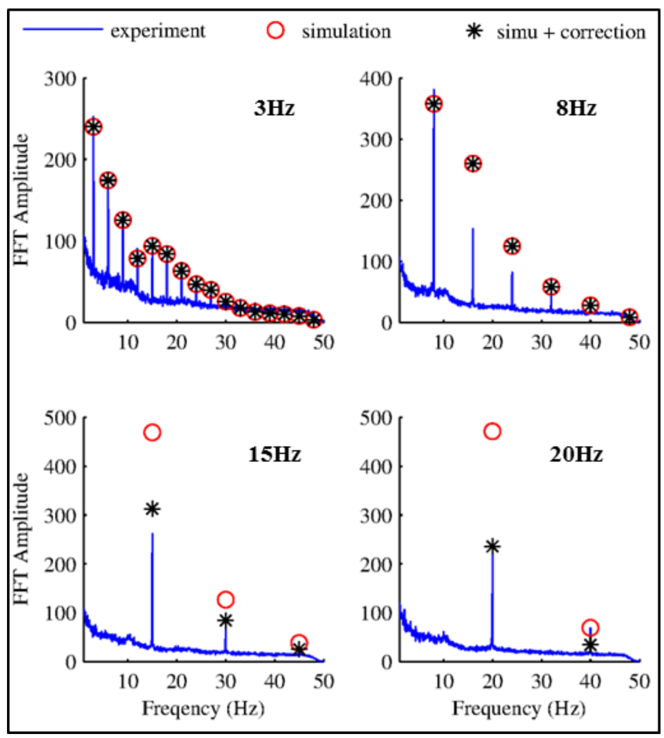

Figure 4. Results of the spectral simulation at different frequencies (3 Hz, 8 Hz, 15 Hz, 20 Hz). Each plot shows the FFT spectrum obtained experimentally during flickering stimulation (blue line), the expected amplitudes obtained by FFT of simulated trains of VEPs (red circles) and the expected amplitudes obtained using the corrected simulation (black stars) (see [II. *H.*]). Note that since the simulation generates signals that are perfectly periodic, the FFT of such signals is equal to zero at every points that are not harmonics of the repetition frequency.

This defines a distance between the two spectra, based only on frequencies at which SSVEP peaks can be found, up to the twentieth harmonic of the stimulation frequency and only if the peak frequency is lower than 40Hz. Results obtained using this distance for each subject and each frequency are shown on Fig. 5 and will be discussed in the next section.

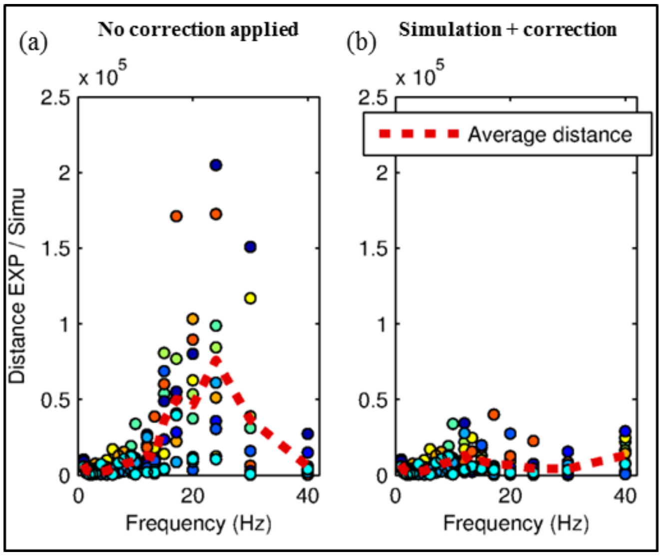

Figure 5. Accuracy of the simulation. (a) and (b) show the distance between the experimental and simulated SSVEP spectra, computed as described in [III. *B*.], using the simple simulation (a) and the corrected simulation (b). Each dot represents one subject at a given frequency. Dots of the same color pertain to the same subject. The red dashed line represents the average distance between experiment and simulation at a given frequency.

IV. Discussion

Fig. 3 shows that the VEP shape and its time-frequency map allow us to make qualitative prediction about the spectral content of SSVEPs. As demonstrated by Fig. 4 and Fig. 5, we can also use VEPs to predict the amplitudes of SSVEP peaks in the Fourier domain quantitatively, using the proposed simulation method. Without any correction, this prediction is very accurate in the 1-6 Hz frequency band, is satisfactory in the 6-12 Hz band, and its accuracy decreases above 12 Hz, with an improvement at 30 Hz and 40 Hz. The corrected version of the simulation algorithm strongly improves the prediction performances in the 15-30 Hz band, while moderately degrading the prediction at 40 Hz.

At low frequencies, good performances of the uncorrected simulation algorithm can be explained by the fact that the SSVEP response is basically a train of VEPs as long as VEPs do not overlap. At such frequencies, FFT components are linked with the shape of the oscillations of the VEP, as illustrated on Fig. 6. On this example, we see that a 16 Hz sine wave with a well-chosen phase overlaps almost perfectly the N65 and P90 components and is in phase with the N180 component. This explains why we observe such a strong oscillatory burst on Fig. 2b centered at (80 ms, 16 Hz), since these components are the most reproducible components of the VEP.

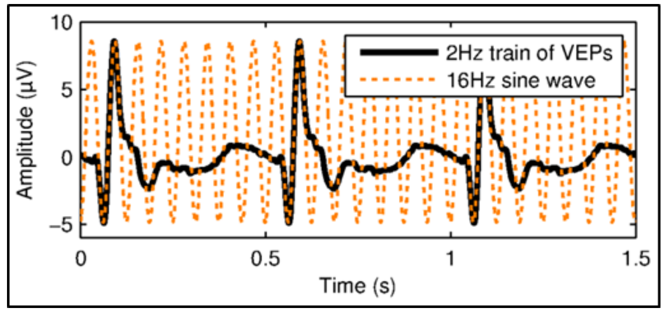

Figure 6. Illustration of why the shape of the VEP explains the strength of the 16 Hz harmonic in SSVEPs generated by a 2Hz flickering stimulation.

At higher frequencies of stimulation, the brain cannot return to (or close to) baseline state before the next VEP is triggered. At frequencies higher than 7 Hz, the N180 of a VEP overlaps with the N65 of the next VEP. Furthermore, at 13 Hz, the P90 component starts to overlap with the following N65. This can be viewed as the source of the low performances of the uncorrected simulation after 13 Hz, and explains why the corrected algorithm gives better results.

The fact that a linear correction to the SSVEP amplitude gave such good results in correcting the prediction in the 15-30 Hz band may give credit to the "brain oscillations" hypothesis against the "phase resetting" hypothesis for event-related potential generation (see [8] for a review of this discussion). Indeed, our simulated SSVEPs are a sum of known brain oscillations (VEPs) even when their amplitude is reduced due to overlapping of two consecutive waveforms. However, better prediction obtained without correction at 40 Hz indicates that our correction strategy may not work for frequencies which are not intrinsically present in the VEP.

From an engineering point of view, being able to predict SSVEP peaks amplitude from VEPs may lead to better calibration of SSVEP detection algorithms, which often only take into account the first two harmonics of the stimulation frequency. This work may therefore lead to an increase of the performances of SSVEP-based BCIs.

References

[1] Odom, J. Vernon, et al. "ISCEV standard for clinical visual evoked potentials (2009 update)." *Documenta ophthalmologica* 120.1 (2010): 111-119.

[2] Husain, Aatif M., et al. "Visual evoked potentials with CRT and LCD monitors When newer is not better." *Neurology* 72.2 (2009): 162-164.

[3] D. Regan, *Human Brain Electrophysiology: Evoked Potentials and Evoked Magnetic Fields in Science and Medicine*. Elsevier, 1989.

[4] Di Russo, Francesco, Wolfgang A. Teder-Sälejärvi, and Steven A. Hillyard. "Steady-state VEP and attentional visual processing." *The cognitive electrophysiology of mind and brain (Zani A, Proverbio AM, eds)* (2002): 259-274.

[5] Vialatte, François-Benoît, et al. "Steady-state visually evoked potentials: focus on essential paradigms and future perspectives." *Progress in neurobiology* 90.4 (2010): 418-438.

[6] Kleiner, Mario, et al. "What's new in Psychtoolbox-3." *Perception* 36.14 (2007): 1-1.

[7] Brainard, David H. "The psychophysics toolbox." *Spatial vision* 10.4 (1997): 433-436.

[8] Sauseng, P., et al. "Are event-related potential components generated by phase resetting of brain oscillations? A critical discussion." *Neuroscience* 146.4 (2007): 1435-1444.